Fluorine K-edge X-ray Absorption Spectroscopy of Lead(II) Tetrafluorostannate(II)

Junya Furutani[1], Keisuke Yamanaka[2], Yoshiharu Uchimoto[3], and Yuki Orikasa[1]

1) *Department of Applied Chemistry, Faculty of Life Sciences, Ritsumeikan University, 1-1-1 Noji-Higashi, Kusatsu 525-8577, Japan*
2) *SR center, Ritsumeikan University, 1-1-1 Noji-higashi, Kusatsu, Shiga, 525-8577, Japan*
3) *Graduate School of Human and Environmental Studies, Kyoto University, Sakyo-ku, Kyoto, 606-8501, Japan*

Lead(II) tetrafluorostannate(II) ($PbSnF_4$) exhibits the highest conductivity among the reported fluoride ion conductors. The previous studies analyzed the diffusion mechanism of fluoride ion based on the crystal structure with the diffraction studies and the nuclear magnetic resonance measurements. In this study, the electronic structure of $PbSnF_4$ is investigated using fluorine K-edge X-ray absorption spectroscopy. The composition of Pb causes the electronic structure change of the vacant F-2p orbital which is the hybridized Pb-6s and Sn-5s orbitals. The electronic structure change is related to the tendency of the fluoride ion conductivity in $Pb_{1-x}Sn_xF_4$.

1. Introduction

Solid fluoride ion conductors have been subjects of research from the old days, and have applications for ion selective electrodes and solid electrolytes for sensors[1-3]. In recent years, the number of research as electrolytes for all solid state secondary batteries are also increasing[4]. Lead(II) Tetrafluorostannate(II) ($PbSnF_4$) exhibits the highest conductivity among the reported fluoride ion conductors[5, 6], and the ion conduction mechanism in $PbSnF_4$ has been one of the interesting research topics. The crystal structure of $PbSnF_4$ roughly has α- (monoclinic), β- (tetragonal), and γ- (cubic) phases[7], and the β-phase exhibits excellent conductivity[8]. The previous crystal structure analysis and NMR studies revealed that the fast conduction path of fluoride ion exists in the β-phase[9-15]. In $Pb_{1-x}Sn_xF_4$, the composition of Pb and Sn depends on the crystal structure and conductivity[16], and it has been reported that the highest conductivity appears when synthesized with a nonstoichiometric composition[17]. Although there are many analytical studies from the crystal structure, as far as the authors know, the influence on the fluoride ion conduction from the viewpoint of the electronic structure of the fluorine has not been investigated. The electronic structure of fluorine can be observed by X-ray absorption spectroscopy (XAS), and we can discuss how the electronic structure relates to conductivity. In this study, $Pb_{1-x}Sn_xF_4$ with different composition is synthesized, F K-edge X-ray absorption spectra are measured, and the relation with the conductivity is examined.

2. Experimental

$PbSnF_4$ was synthesized by a mechanochemical milling. In the glove box in an argon atmosphere, starting materials PbF_2 and SnF_2 were weighed and put into a ball mill pot. The molar ratio of Pb:Sn was 68:32, 60:40, 58:32 and 50:50 in this study. The planetary ball-milling treatment was carried out four times with a rotation time of 600 rpm for 180 minutes. The milled PbF_2-SnF_2 powder was transferred to a quartz crucible and fired in a furnace at 400 °C for 1 hour in an argon atmosphere.

XRD measurements were carried out at room temperature with Rigaku Rint-2200 using Cu Kα radiation. The data were collected in the range from $2\theta = 5°$ to 75° and using the step size of 0.01°.

F K-edge XAS measurement was carried out at Ritsumeikan University SR Center BL-2. The powder samples prepared by the mechanochemical milling were mounted on a carbon tape and transported to a vacuum chamber. F K-edge XAS was measured in a total electron yield method. Energy calibration was performed by setting the peak energy of LiF to 692 eV.

3. Results and Discussion

The crystal structure monotonically changes with Pb composition. Fig. 1(a) is the XRD patterns of synthesized $Pb_{1-x}Sn_xF_4$. Although the diffraction lines that cannot be attributed are seen at Pb 50%, they agree well with the orthorhombic *P*4/*nmm* pattern which is the β-phase. Fig. 1 (b) is a plot of the lattice constant and the lattice volume as a function of Pb composition. It is found that the c-axis length increases with increasing Pb composition and the lattice volume increases. This tendency is due to the ionic radius of Pb being larger than Sn[18]. When the crystal structure is same, the lattice volume increases with increasing Pb composition. With the large lattice volumes, the bottleneck of fluoride ion conduction is relaxed, which is advantageous for further improving the conductivity. However, it is reported that conductivity decreases when Pb exceeds 65%[17], and it is considered that there are other factors of fluoride conduction besides the crystal structure.

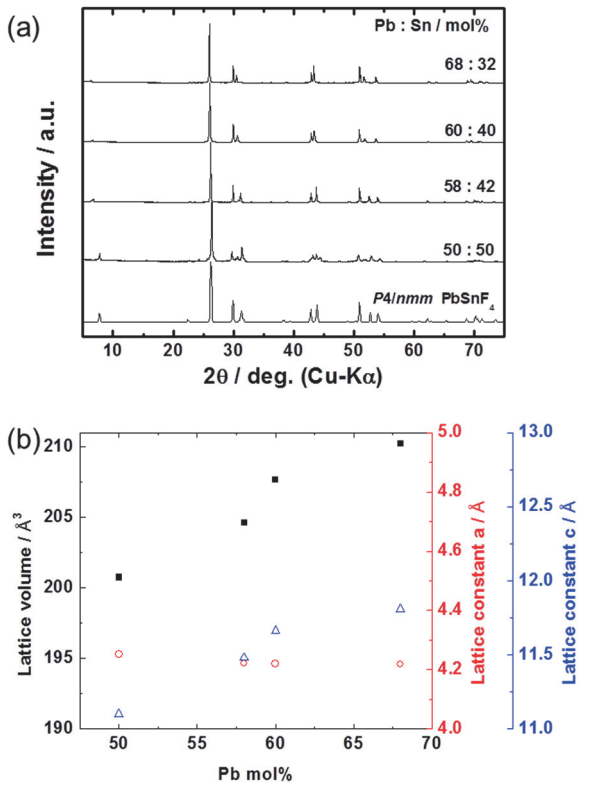

Fig. 1 (a) X-ray diffraction patterns of $Pb_{1-x}Sn_xF_4$. (b) Lattice constant and lattice volume as a function of Pb composition.

The X-ray absorption spectra at F K-edge show a characteristic behavior depending on Pb composition. Figure 2 shows the F K-edge XAS of $Pb_{1-x}Sn_xF_4$ along with the reference samples Pb F_2 and SnF_2. Absorption at F K-edge corresponds to the transition from ground state 1 s orbit to F- 2p empty orbital. This F-2p orbital is hybridized with the Pb-6p orbital and the Sn-5p orbital, and the spectrum shows the state of the hybridized orbital. As indicated by "*a*" and "*b*" in the figure, the two peaks were observed at 686 eV and 688 eV in the first structure, respectively. Although the two peaks can be confirmed in the reference sample PbF_2, it shows a significant energy difference from that of $PbSnF_4$. In SnF_2, only one peak was observed. Therefore, the electronic structure of $PbSnF_4$ cannot be represented by the combination of PbF_2 and SnF_2, which represents the quite different electronic structure.

It seems that the intensity ratio of two peaks varies depending on the composition. For quantitative analysis, the nonlinear curve fitting of the spectra was carried out using the following equation,

$$\mu t = H\left[\frac{1}{2}+\frac{1}{\pi}\arctan\left(\frac{x-P}{\Gamma/2}\right)\right]+a+\sum_i H_i \exp\left[-\frac{1}{2}\left\{\frac{x-P_i}{\Gamma_i/2\sqrt{\ln 4}}\right\}^2\right] \quad (1)$$

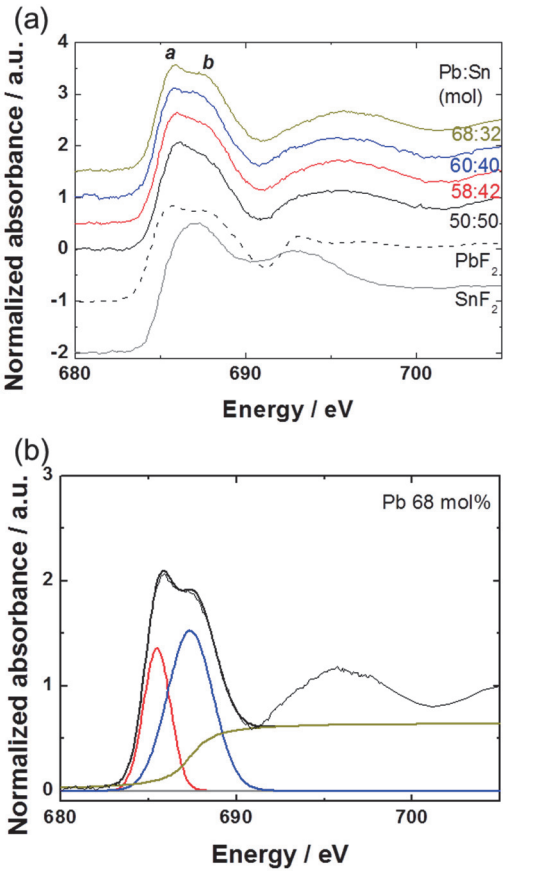

Fig. 2 (a) F K-edge XAS of $Pb_{1-x}Sn_xF_4$ along with the reference samples PbF_2 and SnF_2. (b) Fitted F K-edge XAS spectrum of $PbSnF_4$ (Pb: 68%).

where H_i, P_i, Γ_i, a is the intensity, the position, the half maximum full width of the peak i, and the constant of the background, respectively[19]. The first term represents the background component, and Gauss functional term corresponds to the peak components. One of the fitting results is shown in Fig. 2 (b). Each peak area was calculated from the fitting results. The plot of two peak ratios on the vertical axis and Pb composition on the horizontal axis are shown in Fig. 3. Although the number of plots is small, a volcano-type plot which is maximum when the area of peak *b* is 60 mol% was obtained. The reported conductivity of $Pb_{1-x}Sn_xF_4$ was plotted on the same graph. The conductivity shows the behavior of the volcanic type which becomes maximum when Pb is 62 mol%, and it shows a good agreement with the behavior of the ratio of the peak area of F K-edge measured this time. From the above, it was shown that the electronic structure of fluorine might have a relation to the fluoride ion conductivity. As for the result of this time, in the electronic structure with high conductivity, the increase of the peak *b*, that is, the peak *a* tends to decrease. This is because hybridization with Pb-6p and Sn-5p decreases or electrons are occupied in the lower part of the

conduction band, and the vacant orbital is decreased. Although this result indicates that the electronic structure of fluorine is one of the important parameters, the detailed mechanism is not understood yet. The further analysis using density functional calculations which discuss the relationship between conductivity and electron density change when the composition of $PnSnF_4$ changes is needed.

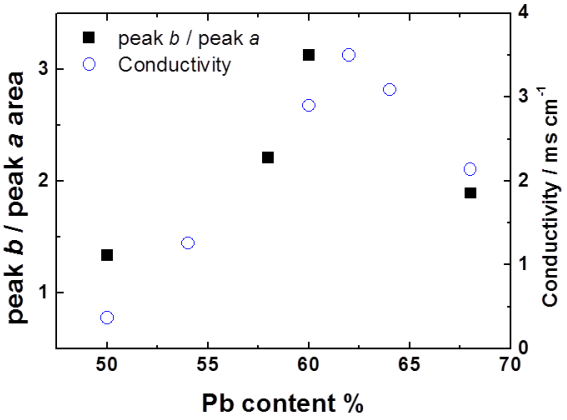

Fig. 3 Calculated peak area ratio of F K-edge XAS of $PbSnF_4$ as a function of Pb composition. For comparison, the conductivity data is plotted from the literature[17].

4. Conclusions

$Pb_{1-x}Sn_xF_4$ of the different constitution was synthesized and the electronic structural change was analyzed by F K-edge XAS. While a monotonically crystal structure change is indicated with Pb composition, possibility of the volcano-type behavior with the two peaks in XAS is indicated, corresponding to the maximum fluoride ion conductivity. The further analysis of the relationship between electronic structure change fluoride ionic conductivity can give us a guideline of the fluoride conduction.

References

(1) T. Eguchi, S. Suda, H. Amasaki, J. Kuwano, Y. Saito, *Solid State Ionics*, **1999**, *121*, 235.
(2) W. Moritz, J. Szeponik, F. Lisdat, A. Friebe, S. Krause, R. Hintsche, F. Scheller, *Sens. Actuator B-Chem.*, **1992**, *7*, 497.
(3) N.I. Sorokin, B.P. Sobolev, *Crystallography Reports*, **2007**, *52*, 842.
(4) F. Gschwind, G. Rodriguez-Garcia, D.J.S. Sandbeck, A. Gross, M. Weil, M. Fichtner, N. Hörmann, *J. Fluorine Chem.*, **2016**, *182*, 76.
(5) J.-M. Réau, C. Lucat, J. Portier, P. Hagenmuller, L. Cot, S. Vilminot, *Mater. Res. Bull.*, **1978**, *13*, 877.
(6) L.N. Patro, K. Hariharan, *Solid State Ionics*, **2013**, *239*, 41.
(7) G. Pérez, S. Vilminot, W. Granier, L. Cot, C. Lucat, J.-M. Réau, J. Portier, P. Hagenmuller, *Mater. Res. Bull.*, **1980**, *15*, 587.
(8) R. Kanno, S. Nakamura, K. Ohno, Y. Kawamoto, *Mater. Res. Bull.*, **1991**, *26*, 1111.
(9) Y. Ito, T. Mukoyama, H. Funatomi, S. Yoshikado, T. Tanaka, *Solid State Ionics*, **1994**, *67*, 301.
(10) R. Kanno, K. Ohno, H. Izumi, Y. Kawamoto, T. Kamiyama, H. Asano, F. Izumi, *Solid State Ionics*, **1994**, *70*, 253.
(11) M.M. Ahmad, K. Yamada, T. Okuda, *J. Phys.-Condes. Matter*, **2002**, *14*, 7233.
(12) M. Castiglione, P.A. Madden, P. Berastegui, S. Hull, *J. Phys.-Condes. Matter*, **2005**, *17*, 845.
(13) E. Murray, D.F. Brougham, J. Stankovic, I. Abrahams, *J. Phys. Chem. C*, **2008**, *112*, 5672.
(14) F. Fujisaki, K. Mori, M. Yonemura, Y. Ishikawa, T. Kamiyama, T. Otomo, E. Matsubara, T. Fukunaga, *J. Solid State Chem.*, **2017**, *253*, 287.
(15) M. Murakami, Y. Morita, M. Mizuno, *J. Phys. Chem. C*, **2017**, *121*, 2627.
(16) M. Uno, M. Onitsuka, Y. Ito, S. Yoshikado, *Solid State Ionics*, **2005**, *176*, 2493.
(17) M. Morita, Y. Uchimoto, Z. Ogumi, Japan Patent, **2017**, JP2017-88427A.
(18) R.D. Shannon, *Acta Crystallogr. Sect. A*, **1976**, *32*, 751.
(19) J. Stöhr, NEXAFS spectroscopy, Springer-Verlag, Berlin, 1992.